JREE: Vol. 6, No. 1, (Winter 2019) 21-28

Journal of Renewable Energy and Environment

Research Article

Journal Homepage: www.jree.ir

Equivalent Electrical Circuit Modeling of Ceramic-Based Microbial Fuel Cells Using the Electrochemical Impedance Spectroscopy (EIS) Analysis

Vajihe Yousefi[a], Davod Mohebbi-Kalhori[a, b*], Abdolreza Samimi[a]

[a] *Department of Chemical Engineering, Faculty of Engineering, University of Sistan and Baluchestan, Zahedan, Iran.*
[b] *Institute of Renewable Energy, University of Sistan and Baluchestan, Zahedan, Iran.*

PAPER INFO

Paper history:
Received 21 June 2019
Accepted in revised form 21 October 2019

Keywords:
Microbial Fuel Cell
Domestic Wastewater
Ceramic Membrane
Gerischer Element
Constant Phase Element

ABSTRACT

The effect of the thickness of ceramic membrane on the productivity of microbial fuel cells (MFCs) was investigated with respect to the electricity generation and domestic wastewater treatment efficiencies. The thickest ceramic membrane (9 mm) gained the highest coulombic efficiency (27.58±4.2 %), voltage (681.15±33.1 mV), and current and power densities (447.11±21.37 mA/m^2, 63.82±10.42 mW/m^2) compared to the 6- and 3-mm thick separators. The results of electrochemical impedance spectroscopy (EIS) analysis were investigated to identify the internal resistance constituents by proposing the appropriate equivalent electrical circuit. The Gerischer element was modeled as the coupled reaction, and diffusion in the porous carbon electrodes and the constant phase element was assimilated into the electrical double-layer capacitance. The thickest ceramic (9 mm) was found to have the largest ohmic resistance; however, owing to its superior barrier capability, it provided more anoxic conditions for better accommodation of exoelectrogenic bacteria in the anode chamber. Therefore, lower charge transfer, fewer diffusional impedances, and higher rates of anodic reactions were achieved. Excessive oxygen and substrate crossover through the thinner ceramics (of 6 and 3 mm) resulted in the suppressed development of anaerobic anodic biofilm and the accomplishment of aerobic substrate respiration without electricity generation.

1. INTRODUCTION

Microbial Fuel Cells (MFCs) are bio-electrochemical systems that can produce electricity by oxidizing waste materials. In today's world entangled with energy and water crises, this technology can address several issues concurrently [1, 2]. Therefore, an understanding of the prominent influencing parameters about the performance of MFCs is of great importance. Formerly, the internal resistance of electrochemical systems was calculated based on the earlier simple methods including the polarization test, which was implemented based on Ohm's law, or current interruption method. However, these methods can only estimate the ohmic resistance of the system and are not adequately accurate in interpreting highly complicated bio-electrochemical systems such as MFCs in which the polarization or charge transfer resistances become as crucial as the ohmic resistance [3].

EIS is a well-established and practical electrochemical technique that can provide comprehensive information about the internal phenomena of MFCs. The identification of these interior phenomena can reveal the role of pivotal affecting parameters in the performance of MFC systems. EIS assessment technique can be implemented for the determination of internal resistance contributors [3-6], optimization of MFC design [7] or operational conditions [8, 9], and biofilm characterization [10-13].

Previously, different thicknesses of two commercial ceramic types have been investigated in the MFC systems with respect to their electricity generation and wastewater treatment performance. However, the internal resistance components of the MFCs were not inspected thoroughly by interpreting the EIS results [14]. The ceramic separator was adopted owing to its several outstanding specifications: enhanced mechanical and chemical stability, accessibility, and low cost, which are necessary for large-scale applications of MFCs [14-18]. In the present research, three different thicknesses of commercial ceramics are utilized to separate the chambers of MFCs. The electricity generation and wastewater treatment capability of the MFCs are studied carefully. Complementary electrochemical analyses including the electrochemical impedance spectroscopy (EIS) and cyclic voltammetry (CV) are carried out, too. The equivalent electrical circuit model (EECM) is introduced to assimilate the impedance responses of EIS analyses for the ceramic-based microbial fuel cells.

2. MATERIALS AND METHODS

2.1. MFC construction and operation

The design of MFCs is identical to that in our previous works [14, 18]. Figure 1 represents the design and components of the MFCs. Carbon cloth is utilized for the fabrication of the electrodes, and stainless steel collectors transmit electricity to the external circuit [18]. Commercial unglazed wall ceramics (Alvand Co., Ghazvin, Iran) with three different thicknesses of 3, 6, and 9 mm split the anode and cathode chambers. The inceptive sample of ceramic is 9 mm thick and is abraded manually to obtain the ceramic membranes with the thicknesses of 3 and 6 mm. The MFCs are named with respect to the thickness of the contained ceramic separators as follows: MFC-9mm, MFC-6mm, and MFC-3mm.

The MFCs are fed by raw domestic wastewater supplied from the septic plant of the University of Sistan and

*Corresponding Author's Email: davoodmk@eng.usb.ac.ir (D. Mohebbi-Kalhori)

Baluchestan. Cathode chamber is empty at first and, then, is gradually filled by the penetrated anodic electrolyte through the ceramic separators. Cathode aeration starts when the catholyte takes up about 30 percent of the cathodic volume [18].

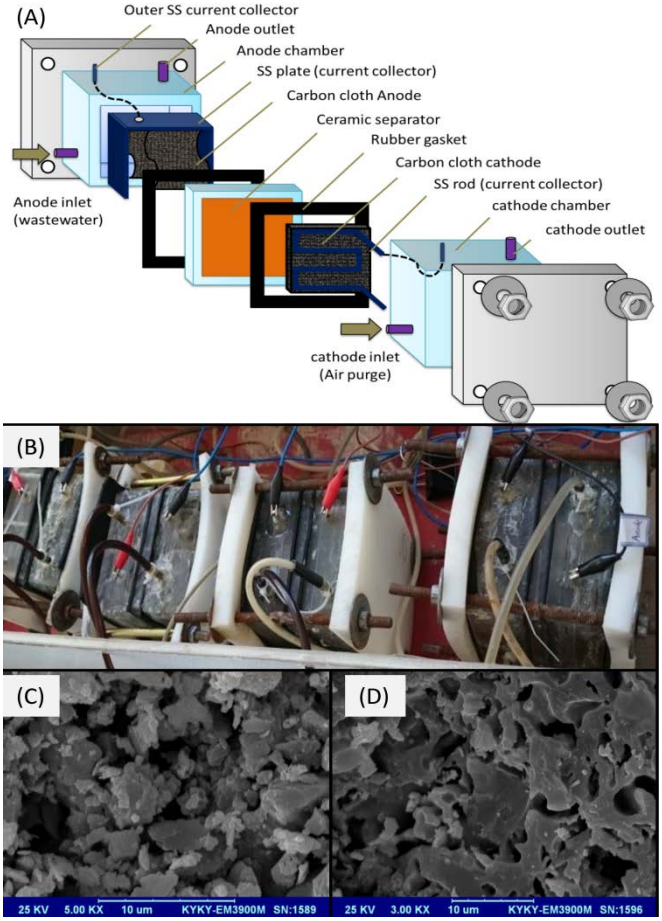

Figure 1. (A) the MFC components [18]; (B) the assembled MFCs that are placed in the box with the controlled temperature; (C) the surface, and (D) cross-sectional SEM images of the ceramic separator.

2.2. Analysis and calculations

The voltage and current (R_{ext}=100 Ω) were regularly recorded by an automatic data acquisition system (USB-4704, Advantech Co., Ltd). Polarization tests were carried out manually by changing the external resistance in the range of 45000-10 Ω and calculating the current and power densities according to Ohm's Law. EIS analyses (OCP, two electrodes, 1 MHz-5 mHz, 10 mV amplitude) and CV (-1.0 to +1.0 V, 0.1 V/s) were carried out by the Autolab PGSTAT302N potentiostat instrument (Metrohm). The NOVA software (*v1.11*) was used to analyze the obtained EIS spectra and determine the internal resistance constituents. The proton conductivity of ceramics (σ, S) was calculated based on the ohmic resistance (R_s, Ω), membrane thickness (L, cm), and surface area (A, cm^2) [18]:

$$\sigma = \frac{L}{R_s A} \quad (1)$$

The coulombic efficiency (CE) was defined as the fraction of theoretical acquirable coulombs, obtained experimentally in the start-up period [14, 18, 19].

Wastewater treatment efficiency was assessed by the variations of COD and BOD, measured using AQUALYTIC AL250 Photometer & CSB/COD- AL38 Reactor, and OxiTop®IS BOD Measuring Device. SEM (LEO 1455VP), XRF (ED 2000, OXFORD), and XRD (Bruker Advance D8) analyses were performed to characterize the ceramic separators. Moreover, ceramic's porosity (ASTM C373-88) and oxygen diffusion coefficient (K_o, cm/s) were determined, as described earlier [18].

3. RESULTS AND DISCUSSION

3.1. Ceramic characterization

The SEM images of the surface and the cross-section of the ceramic membrane are respectively depicted in Figurers 1 C and D. The ceramics are characterized by relatively uniform surface and cross-sectional structures with the pore sizes between 4 to 10 microns and the porosity of 28.94±1.61 %. According to the results of XRF analysis, the major components of ceramic biscuit are SiO_2, Al_2O_3, and CaO with 68.46, 10.95, and 7.23 weight percentages (W/W %), respectively. The predominant crystalline phases of the ceramic biscuit are Quartz, low (Card No. 01-085-0335), and feldspar groups based on the results of XRD analysis [18]. The measured oxygen mass transfer coefficients (K_o, cm/s) are 6.45×10^{-4} cm/s, 8.59×10^{-4} cm/s, and 10.66×10^{-4} cm/s for 9, 6, and 3 mm thick ceramic separators, respectively. The oxygen diffusion rate through the ceramic almost linearly increased as the thickness of ceramic decreased from 9 mm to 3 mm. Since the porosity of all ceramic separators in the present study was the same, their oxygen diffusion coefficients were only controlled by the thickness of ceramic separators. Hence, as expected, the reduction of ceramic thickness eventuated in the increment of oxygen and electrolyte permeability through the membrane.

3.2. Electricity generation

The currents and voltages of the MFCs were recorded automatically using the data acquisition system at defined time intervals. Figure 2 depicts the growing electricity generation trends of the MFCs during the start-up time. The feeding domestic wastewater contained many different types of microorganisms at first; however, gradually, their facultative anaerobic species were dominated by other types due to the anoxic conditions in the anode chamber. A certain type of these facultative anaerobic bacteria, named exoelectrogens or electrochemically active bacteria (EAB), can generate electrons from the oxidization of organic substrates of wastewater, which may be transferred to the electrodes by different extracellular electron transfer (EET) mechanisms [20]. The generated voltages and currents of the MFCs will grow up as the number of EAB in the anode chamber increases. The biofilm becomes matured when these electron-producing types of bacteria constitute the major parts of anodic biofilm; consequently, relatively stable voltage and current are produced.

As depicted in Figure 2, the electricity generation of the MFC-9mm steadily increased until it was stabilized after about 50 hours. While the other MFCs did not yield considerable voltages and currents after the duration of a relatively long period (about 40 hours), probably due to the growth of aerobic or facultative bacteria in the anode chamber. Moreover, the excessive oxygen concentration in the

anode chamber hindered the electron transmission to the cathode via the external circuit, since the oxygen reduction reaction was performed in the anode chamber without any electricity generation. After 40 hours, the aeration in the cathode chambers of MFC-3mm and MFC-6mm ceased reducing the soluble oxygen concentration in the cathode (the time indicated by arrows in Figure 2). Interestingly, the electricity generation of these two MFCs raised drastically afterward, which affirmed the significant impact of oxygen concentration on the performance of MFCs, as well as the insufficient oxygen barrier capability of a thin porous ceramic separator.

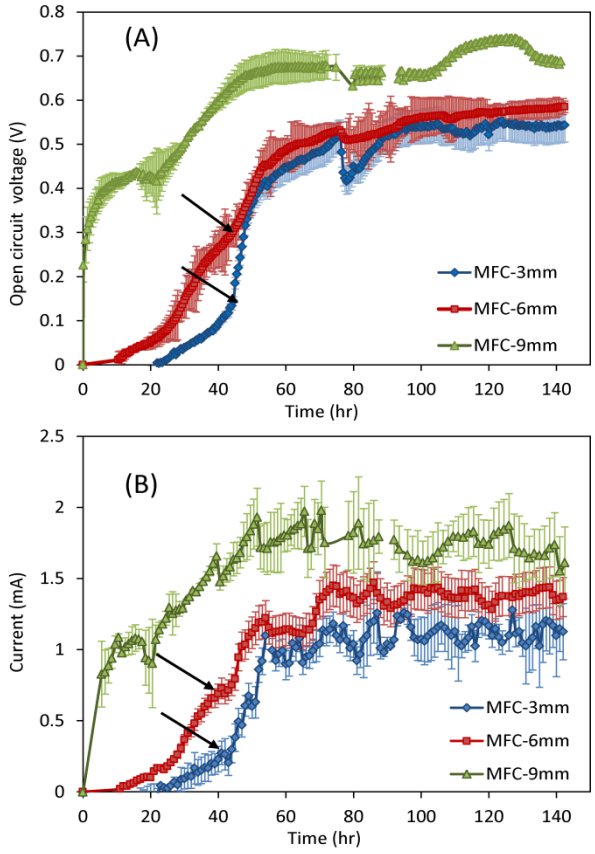

Figure 2. Eelectricity generation during the start-up period: (A) Open circuit voltage and (B) Current production; arrows indicate the time that cathode aeration stopped for the MFC-3mm and the MFC-6mm.

Maximum OCV, current, and coulombic efficiencies (CE) of the MFCs are compared in Table 1. Notwithstanding the ceased cathode aeration, the maximum voltages and currents of the MFC-3mm and the MFC-6mm are lower than the values of the MFC-9mm (P-value<0.05). Tukey post-hoc analysis was performed to statistically assess the difference between the obtained values. The CE of the MFC-9mm is also significantly higher than that of the other two MFCs, thanks to the lower oxygen transmission rate of the thicker ceramic separator. Distinctly, ceramic thickness has a serious influence on the rate of oxygen transfer through the separator and, thereby, on the overall performance of the MFCs.

3.3. Polarization results

The polarization tests were performed after the stabilization of current and voltage (140 h) by changing the external resistor and recording the generated current values in each resistance. The polarization results of the MFCs are presented in Figure 3. The obtained peaks of power and current densities (MPD, MCD) are summarized and compared with the Nafion membrane [14] in Table 1. The power and current generation of the MFCs declined by decreasing the ceramic thickness. The maximum power generation of the MFC-9mm is nearly 1.8 and 1.5 times higher than the values of the MFC-3mm and the MFC-6mm, respectively. Inconsistent with the present results, Behera and Ghangrekar (2011) found that increasing the thickness of earthen pot separators led to higher internal resistance and lower power production of the batch-fed MFCs. However, it must be considered that their thinnest earthen plate separator, which acquired the highest power density, had an acceptable oxygen mass transfer coefficient of 1.79×10^{-5} cm/s, which can fairly control the oxygen diffusion to the anode chamber [21], while the oxygen barrier feature of our thinner ceramic separators is not enough to adequately prevent unwanted aerobic respiration of substrates in the anode compartment (Section 3.1). Hence, the thickest ceramic, despite its higher ohmic resistance, obtained better power generation due to the lower oxygen mass transfer coefficient compared to the other thinner ceramics. Similarly, Khalili et al. (2017) who investigated the performance of MFCs containing the commercial ceramic separators obtained the best power performance for the thickest unglazed wall ceramic separator [14].

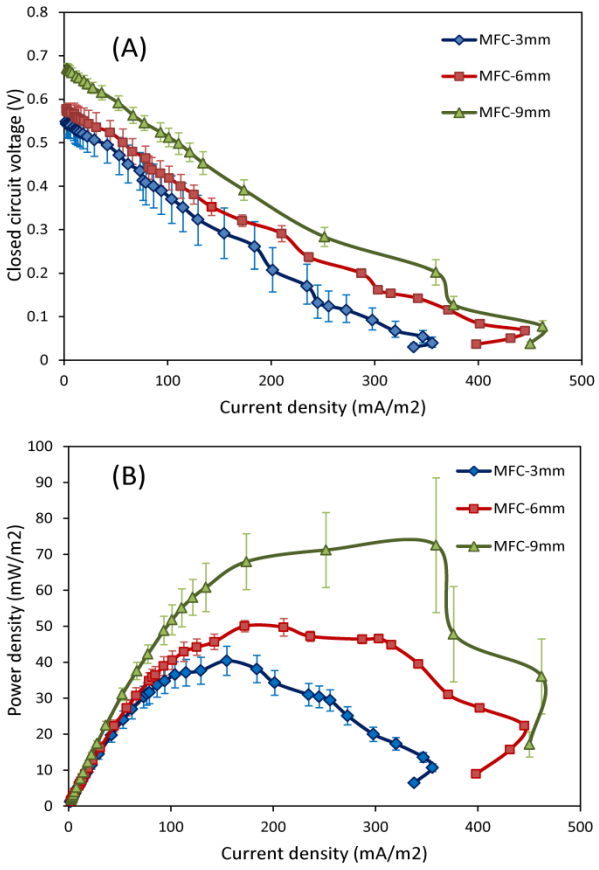

Figure 3. Polarization results of the MFCs: (A) the closed-circuit voltage and (B) the power density versus the current density.

3.4. Wastewater treatment

The COD and BOD removal efficiencies of the MFCs are reported in Table 1. The sewage treatment efficiency was

slightly amended by the reduction of membrane thickness, probably owing to the superimposed aerobic respirations onto the anaerobic approach of wastewater treatment. Similarly, Winfield et al. [22] reported that the increase of electro-osmotic moisture movement through the ceramic membrane in the continuous feeding of air-cathode MFCs not only eliminated the need for the cathode hydration, but also resulted in the improved wastewater treatment efficiency. In this context, Jana et al. [23] and Jadhav et al. [24] introduced innovative MFC designs in which the anodic effluents were conveyed to the cathode chamber to enhance the treatment efficiency by adding an aerobic treatment step.

Table 1. The overall performance of the MFCs regarding the electricity generation and wastewater treatment efficiency.

MFC	OCV (mV)	Current (mA)	MPD (mW/m^2)	MCD (mA/m^2)	CE (%)	COD (%)	BOD (%)
MFC-9mm	681.15±33.1	1.91±0.3	72.54±10.42	462.22±21.37	27.58±4.2	88.58	86.11
MFC-6mm	585.7±14.2	1.47±0.5	50.01±8.1	445.33±21.4	15.56±2.9	97.67	98.33
MFC-3mm	562.5±16.4	1.28±0.8	40.37±19.2	355.56±13.2	10.77± 0.8	97.75	97.96
Nafion 117 [14]	856	5.03 ±16	602	1750	53.0	85	86.11

3.5. Electrochemical impedance spectroscopy (EIS)

EIS analysis can be carried out in either two-electrode or three-electrode connection modes depending on the objective of an experiment. Two-electrode configuration is desirable for measuring the components of internal resistance, and the three-electrode mode is used for studying individual electrodes more accurately [3]. In this study, the two-electrode connection was selected, and each EIS experiment was implemented twice. Firstly, the anode adopted as the working electrode, and the cathode was connected to both the counter and reference ports; then, the working electrode was displaced in the second test. The individual constituents of internal resistance were generally estimated by adjusting an appropriate equivalent electrical circuit (EEC) to the experimental impedance data. Commonly, an EEC is the combination of typical electrical elements that can elucidate the interior system phenomena and produce the same impedance results.

In general, the maximum generated voltage of an MFC is lower than the theoretical attainable value owing to the overpotential of the electrodes as well as the ohmic losses [25, 26]. In the modeling of an MFC system by EEC, the electrode overpotential was customarily assimilated with a parallel resistor and capacitor, representing the electrode's charge transfer impedance (R_{ct}) and the capacitance of electrical double layer (EDL), respectively. The "electrical double layer" with the oppositely charged ions is usually developed next to the electrode surface, simulated with a capacitor for the ideal smooth electrodes and with a constant phase element (CPE) in the case of non-homogeneous or distributed nature of surface or reactions on the electrode surface [27]. In the present study, CPE was adopted for the double-layer capacitance of electrodes due to both the non-uniformity of carbon cloth surface with distributed active sites and the pseudo-capacitive nature of bio-electrochemical reactions.

Moreover, diffusion or mass transfer resistance must also be considered in the polarization impedance of porous electrodes. Different diffusional elements were used for distinct physical situations, including the distributed Warburg element (W) for infinite or semi-finite diffusion, Tangent and Cotangent hyperbolic (T and O) elements for thin layer diffusions and Gerischer element (G) for accompanied diffusion and reaction occasions. The Gerischer element is derived from the most general diffusion model in which the modified Fick's law was coupled with the related kinetic parameters, which can be logically applied for modeling porous electrodes.

The proposed equivalent circuit for the ceramic-based MFC systems (inset in Figure 4) was fitted to the experimental EIS data using the NOVA software by the minimization of chi-square (χ^2) parameter. Moreover, the Kramers-Kronig test has been performed to ensure data compliance with the requisite conditions of stability, linearity, causality, and finiteness for all frequency ranges [28, 29]. The experimental and the fitted impedances of EIS analyses are depicted in Figure 4.

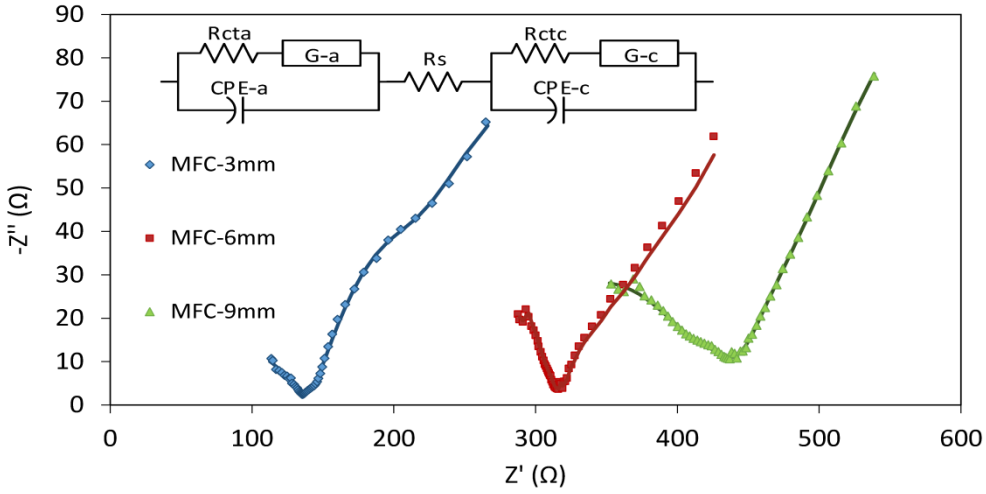

Figure 4. Experimental (points) and fitted (lines) values obtained from the electrochemical impedance spectroscopy (EIS) analyses; the inset shows the proposed equivalent electrical circuit for the simulation of the MFC systems.

The obtained ohmic resistances of the MFCs are summarized in Table 2. Consistent with the results of previous research studies [14, 21], the ohmic resistance (R_s) considerably decreased by the reduction of ceramic separator thickness. The higher thickness of ceramic membrane resulted in the increase of the distance between the electrodes and the elongation of the proton diffusion path. Moreover, since domestic wastewater has low conductivity, increasing the electrodes distance can significantly raise the ohmic resistance.

The proton conductivity of each ceramic separator was calculated with respect to the obtained ohmic resistance and physical specifications of the membrane. As can be seen in Table 2, the proton conductivity of the membranes was reduced by increasing the ceramic thickness.

Table 2. The ohmic resistance and the charge transfer impedances of the MFCs.

MFC	R_s (Ω)	R_{cta} (Ω)	R_{ctc} (Ω)	σ (μS/cm)
MFC-3mm	38.53±3.97	236.84±9.93	15.69±2.95	417.45±43.04
MFC-6mm	100.10±14.9	209.78±8.98	10.69±0.83	107.77±16.12
MFC-9mm	248.72±0.24	184.89±1.91	6.97±0.27	66.57±3.22

Although thickening the ceramic separator increased the ohmic resistance, the charge transfer impedance of the anode electrode (R_{cta}) decreased as a result. The better oxygen barrier ability of the thicker ceramics provides a more anaerobic anodic environment for the growth of exoelectrogenic bacteria, which can reduce the charge transfer resistance owing to their bio-catalytic nature. Borole et al. (2010) showed that the anodic charge transfer impedance of MFCs effectively decreased from 296.1 to 36.3 Ω by the development of the EAB biofilm during the first 43 days of the start-up period [10]. Similarly, Aaron et al. (2010) reported the more drastic decrement of the anodic charge transfer impedance from 315±12 to 3.75±0.30 Ω over the first five days of the MFC operation as a result of the propagation of exoelectrogen biofilm. The anodic impedance remained almost stable afterward. They concluded that the rapid decrease of the anodic impedance was attributed to the origin of the anode inoculum, which was obtained from a matured MFC [9]. Hence, the lower anodic charge transfer impedance of the MFC-9mm compared to the other two MFCs demonstrates better accommodation of electrochemically active bacteria in the anode of this MFC.

The cathodic charge transfer impedance of the MFCs is similarly decreased by thickening the ceramic biscuit membranes (Table 2). Presumably, the lower electrolyte permeation through the thicker ceramic helps better growth and attachment of the cathodic biofilm to the electrode, which consequently reduced the cathodic charge transfer impedance.

The capacitance of the electrical double layer (EDL) can reveal both the quality and the quantity of developed biofilms nearby the electrode surface. CPE is a non-intuitive circuit element, which is introduced to assimilate the EDL adjacent to the non-homogenous surface of porous carbon cloth electrodes, and is mathematically defined in Equation (2):

$$Z_{CPE}(\omega) = \frac{1}{(j\omega)^{\alpha}Q} \quad (2)$$

where j and ω represent the imaginary unit and the angular frequency ($\omega=2\pi f$, f is the frequency in Hz), respectively. α and Q ($F.s^{\alpha-1}$ or $S.s^{\alpha}$) are frequency-independent constants of CPE. When α is close to one, CPE resembles a capacitor with the constant phase of (90×α) in all frequency ranges; in the case of α=1, the equation of CPE is the same as a perfect capacitor. For α=0, CPE acts as a resistor, and for α=-1, it represents the same behavior of an inductor [30]. The application of CPE in modeling microbial electrochemical cells (MECs) has already grown owing to the biological nature of electrochemical reactions and their usually porous structure of electrodes [9, 10, 31, 32]. Several formulas have been introduced yet to calculate the effective or interfacial EDL capacitance from the CPE parameters of α and Q [31, 33, 34]. Brug's equation has been widely used in the literature for estimating the interfacial capacitance (C_{DL}) of the surface distributed time constants (Eq. 3) [35]:

$$C_{DL} = \left[Q(R_s^{-1} + R_{ct}^{-1})^{(\alpha-1)}\right]^{1/\alpha} \quad (3)$$

where R_s and R_{ct} are the electrolyte and the charge transfer impedances, respectively. The obtained constants of CPE elements for the anode and cathode electrodes and their calculated effective double-layer capacitance are listed in Table 3.

The EDL capacitance of the anode electrode remarkably improved by thickening the ceramic separator. It was demonstrated that propagating the biofilm over the electrode surface increased the double-layer capacitance owing to the presence of c-type cytochromes in a living, electrically conductive biofilm [36].

Table 3. The CPE parameters obtained from EEC modeling along with the calculated capacitance of the electrical double layers next to the electrodes.

MFC	CPE-anode			CPE-cathode		
	$Q\times10^{-5}$	α	C_{DL} (nF/cm^2)*	$Q\times10^{-5}$	α	C_{DL} (nF/cm^2)*
MFC-3mm	5.82±0.63	0.36±0.005	$2.42\times10^{-3}\pm2.7\times10^{-4}$	50.57±1.49	0.34±0.02	0.16±0.01
MFC-6mm	9.22±0.16	0.40±0.01	0.103±0.019	51.19±0.86	0.45±0.001	3.06±0.26
MFC-9mm	13.67±0.69	0.45±0.01	1.46±0.21	48.14±3.1	0.58±0.29	74.32±1.2

* The double layer capacitances (C_{DL}) of the anode and cathode electrodes are normalized by the superficial surface area of each electrode (480 cm^2 and 262.5 cm^2 for the anode and the cathode, respectively).

Therefore, the higher double-layer capacitance indicates the presence of a thicker or denser living biofilm on the anode surface of the MFC-9mm. Excessive oxygen permeation through the thinner ceramic membranes prevents the growth and development of an EAB biofilm over the anode electrode. Moreover, it must be considered that this little anodic double-layer capacitance for the MFC-3mm was acquired with no cathode aeration.

Besides, the value of α can represent the degrees of non-ideality of CPE in general. Moreover, it was previously reported that by increasing the time of inoculation and development of anaerobic EAB bacteria in the anode compartment, the value of α increased consequently until reaching nearly one for matured biofilm [9, 10]. The higher value α of the CPE-anode for the MFC-9mm demonstrated that the thickest ceramic separator could provide better anoxic conditions for the growth of the facultative anaerobic electron-producing bacteria in the anode chamber compared to the MFC-6mm and MFC-3mm. These results denote the crucial effect of oxygen concentration on the growth of exoelectrogenic biofilm in the anode chamber.

The double-layer capacitance of the cathode electrodes similarly increased by thickening the ceramic membrane and, then, reached the maximum for the MFC-9mm, which indicates a denser biofilm over the cathode of this MFC. Presumably, a high rate of electrolyte permeation through the thinner ceramics prevented biofilm development over the cathode surface.

On the other hand, the coupled diffusion and reaction phenomena in the porous electrodes were defined by the Gerischer element (Eq. 4):

$$Z_G(\omega) = \frac{1}{Y_0\sqrt{k + j\omega}} \quad (4)$$

where Y_0 (S) is the admittance of the Gerischer element, and k shows the overall rate constant of all reactions performed on the electrodes. The obtained values for the Gerischer elements of the anode and the cathode electrodes are shown in Table 4. The overall anodic reaction rate (k-Gerischer-anode) was fallen by decreasing the ceramic thickness. Seemingly, the lower thickness of ceramic separator did not have sufficient oxygen barrier capability to provide the anaerobic condition in the anode chamber; thereby, the overall rate of anodic reactions was influenced by the high concentration of oxygen in the anode compartment.

Investigating the effective reaction rate constant of the cathode (k-Gerischer-cathode) revealed that decreasing the thickness of the ceramic separator from 9 to 6 mm increased the rate of cathodic reactions. Probably, the lower thickness of ceramic in the MFC-6mm resulted in the higher permeation of anodic electrolyte to the cathode. Thereby, the higher portion of wastewater respiration was performed in the cathode chamber without any contribution to the electricity generation of the MFC-6mm. Furthermore, it can be seen that the elimination of cathode aeration in the MFC-3mm reduced the rate of aerobic cathodic reactions considerably. Moreover, the excessive electrolyte leak through the thin ceramic may limit the growth of aerobe biofilm over the cathode surface of the MFC-3mm.

The anodic Gerischer admittance was amended by increasing the ceramic thickness. Therefore, the anodic diffusional resistance decreased by thickening the ceramic separator, presumably due to the better development of the EAB biofilm over the anode surface. The Gerischer admittance of the cathode similarly increased for the MFCs containing the thicker ceramic membrane. This may occur owing to the presence of denser cathodic biofilm as corroborated by increasing the double-layer capacitance nearby the cathode electrodes of MFCs with the thicker membrane.

Figure 5 shows the effect of ceramic membrane thickness on each component of the internal resistance. In spite of its higher ohmic resistance, the MFC-9mm has the lowest internal resistance and shows the highest electricity generation performance compared to the MFC-6mm and MFC-3mm. This supremacy was attributed to the reasonable barrier properties of the thicker ceramic separator, which prevented the short-circuiting and resulted in better accommodation and growth of EAB biofilm in the anode chamber, too. The presence of exoelectrogenic biofilm markedly decreased the charge transfer and diffusional impedances and, thereby, reduced the internal resistance of the MFCs.

Table 4. The Gerischer elements and the diffusional impedances of the electrodes.

MFC	Gerischer-anode		$R_{d\text{-anode}}$ (Ω)	Gerischer-cathode		$R_{d\text{-cathode}}$ (Ω)
	$Y_0\times10^{-3}$ (S)	k		$Y_0\times10^{-3}$ (S)	$k\times10^{-3}$	
MFC-3mm	9.87±1.7	0.26±0.01	101.32±2.6	3.89±0.34	6.35±2.4	256.81±3.4
MFC-6mm	23.83±5.3	3.25±0.82	41.97±3.8	4.19±0.004	109.91±14.4	236.66±1.7
MFC-9mm	41.39±4.3	4.45±1.20	24.16±1.4	10.58±0.46	96.84±0.4	94.52±2.5

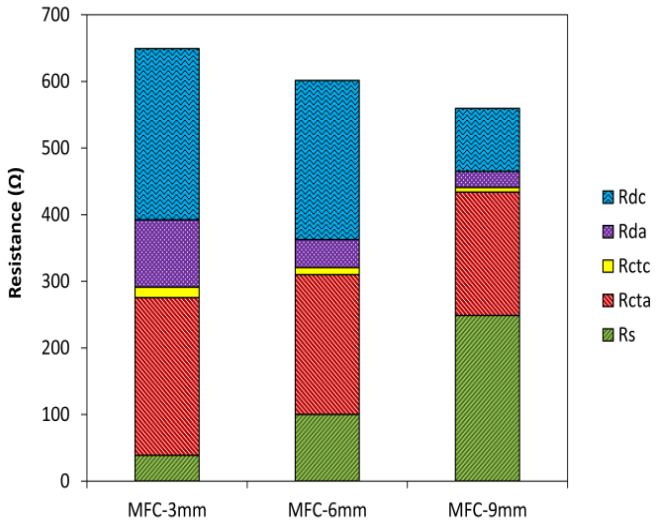

Figure 5. The internal resistance components of the MFCs.

3.6. Cyclic voltammetry

Cyclic voltammetry (CV) is a powerful electrochemical technique for the characterization of various energy-storing devices, including microbial fuel cells. Much beneficial information can be obtained by interpreting the CV results such as investigating the dominant electron transfer mechanisms [37, 38] or calculating the electrical double-layer capacitance nearby the electrodes [39]. The capacitance of electrical double layer (EDL) is calculated by estimating the accumulated charge on the electrode surface during each CV cycle, which can be found by integrating the entrapped surface between the oxidative and reductive potential sweeps of cyclic voltammogram [39]. As depicted in Figure 6, The CV results of ceramic-based MFCs have quite similar sigmoidal shapes without any observable current humps. Decreasing the ceramic thickness from 9 to 6 mm reduced the entrapped surface of CV cycle, which corroborates the drastic decrease of the double-layer capacitance of the electrodes obtained from the EIS results. Furthermore, the maximum current densities of both forward and backward

sweeps of CV curves reduced seriously. Consistent with the electricity generation results and the results of the EIS analyses, the MFC-9mm gained the highest anodic and cathodic current peak in the CV cycle.

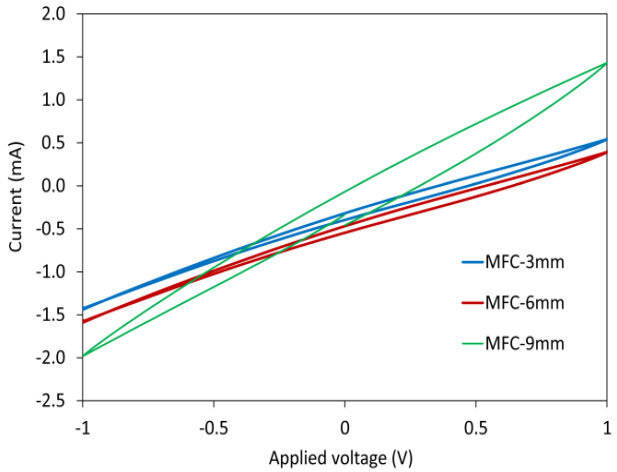

Figure 6. The results of cyclic voltammetry (CV) analyses.

4. CONCLUSIONS

Electrochemical analyses are powerful techniques that can provide valuable information about the interior phenomena of microbial fuel cells (MFCs). In the present study, three different thicknesses (3, 6 and 9 mm) of a commercial unglazed wall ceramic were utilized as the cost-effective separator of continuous MFCs for treating domestic wastewater. Besides investigating electricity generations and wastewater treatment efficiencies, the EIS and CV analyses were implemented, too. The MFC containing the thickest ceramic generated the highest voltage, current, and power densities and the best coulombic efficiency amongst the others. However, it has slightly lower wastewater treatment efficiencies than the thinner ceramic separators. The proposed equivalent electrical circuit contained a Gerischer element (G) for the simulation of coupled diffusion and reaction phenomena in the porous electrodes and a constant phase element (CPE) for assimilating the pseudo-capacitive behavior of anodic biofilm nearby the electrodes. Fitting the EEC on the EIS responses showed that although the thickest ceramic membrane had the highest ohmic resistance, the better barrier capability of this separator provided a more anaerobic environment in the anode compartment and prevented the electrolyte leakage to the cathode chamber. Therefore, lower charge transfer impedances and higher reaction rates are obtained in both the anode and cathode electrodes of the MFC-9mm. While the insufficient barrier ability of thinner ceramic membranes (6 and 3 mm) resulted in (a) the effusively oxygen and substrate transportation between the chambers, (b) the development of unwanted aerobic bacteria instead of anaerobic exoelectrogen biofilm in the anode, and (c) the accomplishment of aerobic degradation of substrates without any electricity generation. Overall, for adopting the optimum thickness of a ceramic membrane, a compromise between decreasing the ohmic resistance and providing adequate barrier capability of the membrane must be considered. The application of the equivalent circuit modeling for the interpretation of EIS data in the present study provided more detailed information about the internal phenomena of the MFCs, which can facilitate a better understanding of the reasons of each alteration and more convenient optimization of the affecting parameters.

5. ACKNOWLEDGEMENT

This research was supported by the University of Sistan and Baluchestan (Grant number 932/2/1006). The authors would like to acknowledge the Alvand Tile and Ceramic Company for kindly providing the ceramic biscuits for this research.

REFERENCES

1. Sen, V., "Should indians pay more for renewable energy based electricity?-The need for evidence based consumer tariffs for electricity in India", ***Journal of Renewable Energy and Environment (JREE)***, Vol. 4, No. 2 and 3, (2017), 23-32.
2. Ameri, M. and Yoosefi, M., "Power and fresh water production by solar energy, fuel cell, and reverse osmosis desalination", ***Journal of Renewable Energy and Environment (JREE)***, Vol. 3, No. 1, (2016), 25-34.
3. He, Z. and Mansfeld, F., "Exploring the use of electrochemical impedance spectroscopy (EIS) in microbial fuel cell studies", ***Energy & Environmental Science***, Vol. 2, No. 2, (2009), 215-219. (https://doi.org /10.1039/B814914C).
4. Manohar, A.K. and Mansfeld, F., "The internal resistance of a microbial fuel cell and its dependence on cell design and operating conditions", ***Electrochimica Acta***, Vol. 54, No. 6, (2009), 1664-1670. (https://doi.org/10.1016/j.electacta.2008.06.047).
5. You, S., Zhao, Q., Zhang, J., Liu, H., Jiang, J. and Zhao, S., "Increased sustainable electricity generation in up-flow air-cathode microbial fuel cells", ***Biosensors and Bioelectronics***, Vol. 23, No. 7, (2008), 1157-1160. (https://doi.org/10.1016/j.bios.2007.10.010).
6. Hosseini, M.G. and Ahadzadeh, I., "Electrochemical impedance study on methyl orange and methyl red as power enhancing electron mediators in glucose fed microbial fuel cell", ***Journal of the Taiwan Institute of Chemical Engineers***, Vol. 44, No. 4, (2013), 617-621. (https://doi.org/10.1016/j.jtice.2013.01.004).
7. Liang, P., Huang, X., Fan, M.-Z., Cao, X.-X. and Wang, C., "Composition and distribution of internal resistance in three types of microbial fuel cells", ***Applied Microbiology and Biotechnology***, Vol. 77, No. 3, (2007), 551-558. (https://doi.org/10.1007/s00253-007-1193-4).
8. He, Z., Huang, Y., Manohar, A.K. and Mansfeld, F., "Effect of electrolyte pH on the rate of the anodic and cathodic reactions in an air-cathode microbial fuel cell", ***Bioelectrochemistry***, Vol. 74, No. 1, (2008), 78-82. (https://doi.org/10.1016/j.bioelechem.2008.07.007).
9. Aaron, D., Tsouris, C., Hamilton, C.Y. and Borole, A.P., "Assessment of the effects of flow rate and ionic strength on the performance of an air-cathode microbial fuel cell using electrochemical impedance spectroscopy", ***Energies***, Vol. 3, No. 4, (2010), 592-606. (https://doi.org/10.3390/en3040592).
10. Borole, A.P., Aaron, D., Hamilton, C.Y. and Tsouris, C., "Understanding long-term changes in microbial fuel cell performance using electrochemical impedance spectroscopy", ***Environmental Science & Technology***, Vol. 44, No. 7, (2010), 2740-2745. (https://doi.org/10.1021/es9032937).
11. Ramasamy, R.P., Ren, Z., Mench, M.M. and Regan, J.M., "Impact of initial biofilm growth on the anode impedance of microbial fuel cells", ***Biotechnology and Bioengineering***, Vol. 101, No. 1, (2008), 101-108. (https://doi.org/10.1002/bit.21878).
12. Chen, B.-Y., Hong, J., Ng, I.S., Wang, Y.-M., Liu, S.-Q., Lin, B. and Ni, C., "Deciphering simultaneous bioelectricity generation and reductive decolorization using mixed-culture microbial fuel cells in salty media", ***Journal of the Taiwan Institute of Chemical Engineers***, Vol. 44, No. 3, (2013), 446-453. (https://doi.org/10.1016/j.jtice. 2012.12.003).
13. Martin, E., Savadogo, O., Guiot, S.R. and Tartakovsky, B., "Electrochemical characterization of anodic biofilm development in a microbial fuel cell", ***Journal of Applied Electrochemistry***, Vol. 43, No. 5, (2013), 533-540. (https://doi.org/10.1007/s10800-013-0537-2).
14. Khalili, H.-B., Mohebbi-Kalhori, D. and Afarani, M.S., "Microbial fuel cell (MFC) using commercially available unglazed ceramic wares: Low-cost ceramic separators suitable for scale-up", ***International Journal of Hydrogen Energy***, Vol. 42, No. 12, (2017), 8233-8241. (http://dx.doi.org/10.1016/j.ijhydene.2017.02.095).
15. Winfield, J., Gajda, I., Greenman, J. and Ieropoulos, I., "A review into the use of ceramics in microbial fuel cells", ***Bioresource Technology***,

Vol. 215, No. (2016), 296-303. (https://doi.org/10.1016/j.biortech. 2016.03.135).

16. Yousefi, V., Mohebbi-Kalhori, D. and Samimi, A., "Ceramic-based microbial fuel cells (MFCs): A review", ***International Journal of Hydrogen Energy***, Vol. 42, No. 3, (2017), 1672-1690. (https://doi.org/ 10.1016/j.ijhydene.2016.06.054).
17. Cheraghipoor, M., Mohebbi-Kalhori, D., Noroozifar, M. and Maghsoodlou, M.T., "Comparative study of bioelectricity generation in a microbial fuel cell using ceramic membranes made of ceramic powder, Kalporgan's soil, and acid leached Kalporgan's soil", ***Energy***, Vol. 178, No. (2019), 368-377. (https://doi.org/10.1016/j.energy. 2019.04.124).
18. Yousefi, V., Mohebbi-Kalhori, D. and Samimi, A., "Application of layer-by-layer assembled chitosan/montmorillonite nanocomposite as oxygen barrier film over the ceramic separator of the microbial fuel cell", ***Electrochimica Acta***, Vol. 283, No. (2018), 234-247. (https://doi.org/10.1016/j.electacta.2018.06.173).
19. Yousefi, V., Mohebbi-Kalhori, D., Samimi, A. and Salari, M., "Effect of separator electrode assembly (SEA) design and mode of operation on the performance of continuous tubular microbial fuel cells (MFCs)", ***International Journal of Hydrogen Energy***, Vol. 41, No. 1, (2016), 597-606. (https://doi.org/10.1016/j.ijhydene.2015.11.018).
20. Kumar, A., Hsu, L.H.-H., Kavanagh, P., Barrière, F., Lens, P.N.L., Lapinsonnière, L., Lienhard, J.H., Schröder, V.U., Jiang, X. and Leech, D., "The ins and outs of microorganism–electrode electron transfer reactions", ***Nature Reviews Chemistry***, Vol. 1, No. (2017), 0024. (https://doi.org/10.1038/s41570-017-0024).
21. Behera, M. and Ghangrekar, M.M., "Electricity generation in low cost microbial fuel cell made up of earthenware of different thickness", ***Water Science & Technology***, Vol. 64, No. 12, (2011). (https://doi.org/10.2166/wst.2011.822).
22. Winfield, J., Greenman, J., Huson, D. and Ieropoulos, I., "Comparing terracotta and earthenware for multiple functionalities in microbial fuel cells", ***Bioprocess and Biosystems Engineering***, Vol. 36, No. 12, (2013), 1913-1921. (https://doi.org/10.1007/s00449-013-0967-6).
23. Jana, P.S., Behera, M. and Ghangrekar, M.M., "Performance comparison of up-flow microbial fuel cells fabricated using proton exchange membrane and earthen cylinder", ***International Journal of Hydrogen Energy***, Vol. 35, No. 11, (2010), 5681-5686. (https://doi.org/10.1016/j.ijhydene.2010.03.048).
24. Jadhav, D.A., Ghadge, A.N. and Ghangrekar, M.M., "Simultaneous organic matter removal and disinfection of wastewater with enhanced power generation in microbial fuel cell", ***Bioresource Technology***, Vol. 163, (2014), 328-334. (http://dx.doi.org/10.1016/j.biortech. 2014.04.055).
25. Logan, B.E., Hamelers, B., Rozendal, R., Schroder, U., Keller, J., Freguia, S., Aelterman, P., Verstraete, W. and Rabaey, K., "Microbial fuel cells: Methodology and technology", ***Environmental Science & Technology***, Vol. 40, No. 17, (2006), 5181-5192. (https://doi.org/ 10.1021/es0605016).
26. Logan, B.E., Microbial fuel cells, John Wiley & Sons, (2008).
27. Barsoukov, E. and Macdonald, J.R., Impedance spectroscopy: Theory, experiment, and applications, John Wiley & Sons, (2005).
28. Strik, D.P., Ter Heijne, A., Hamelers, H.V., Saakes, M. and Buisman, C., "Feasibility study on electrochemical impedance spectroscopy for microbial fuel cells: Measurement modes & data validation", ***ECS Transactions***, Vol. 13, No. 21, (2008), 27-41. (https://doi.org/10.1149/ 1.3036209).
29. Boukamp, B.A., "A linear Kronig-Kramers transform test for immittance data validation", ***Journal of the Electrochemical Society***, Vol. 142, No. 6, (1995), 1885-1894. (https://doi.org/10.1149/ 1.2044210).
30. Jorcin, J.-B., Orazem, M.E., Pébère, N. and Tribollet, B., "CPE analysis by local electrochemical impedance spectroscopy", ***Electrochimica Acta***, Vol. 51, No. 8-9, (2006), 1473-1479. (https://doi.org/10.1016/ j.electacta.2005.02.128).
31. Dominguez-Benetton, X., Sevda, S., Vanbroekhoven, K. and Pant, D. "The accurate use of impedance analysis for the study of microbial electrochemical systems", ***Chemical Society Reviews***, Vol. 41, No. 21, (2012), 7228-7246. (https://doi.org/10.1039/C2CS35026B).
32. Sevda, S., Chayambuka, K., Sreekrishnan, T.R., Pant, D. and Dominguez-Benetton, X., "A comprehensive impedance journey to continuous microbial fuel cells", ***Bioelectrochemistry***, Vol. 106, No. (2015), 159-166. (https://doi.org/10.1016/j.bioelechem.2015.04.008).
33. Hirschorn, B., Orazem, M.E., Tribollet, B., Vivier, V., Frateur, I. and Musiani, M., "Determination of effective capacitance and film thickness from constant-phase-element parameters", ***Electrochimica Acta***, Vol. 55, No. 21, (2010), 6218-6227. (https://doi.org/10.1016/ j.electacta.2009.10.065).
34. Hsu, C.H. and Mansfeld, F., "Technical note: Concerning the conversion of the constant phase element parameter Y0 into a capacitance", ***Corrosion***, Vol. 57, No. 9, (2001), 747-748. (https://doi.org/10.5006/1.3280607).
35. Brug, G.J., van den Eeden, A.L.G., Sluyters-Rehbach, M. and Sluyters, J.H., "The analysis of electrode impedances complicated by the presence of a constant phase element", ***Journal of Electroanalytical Chemistry and Interfacial Electrochemistry***, Vol. 176, No. 1, (1984), 275-295. (https://doi.org/10.1016/S0022-0728(84)80324-1).
36. Malvankar, N.S., Mester, T., Tuominen, M.T. and Lovley, D.R., "Supercapacitors based on C-type cytochromes using conductive nanostructured networks of living bacteria", ***Chemphyschem:An EuropeanJournal of Chemical Physics and Physical Chemistry***, Vol. 13, No. 2, (2012), 463-468. (https://doi.org/10.1002/cphc.201100865).
37. Fricke, K., Harnisch, F. and Schroder, U., "On the use of cyclic voltammetry for the study of anodic electron transfer in microbial fuel cells", ***Energy & Environmental Science***, Vol. 1, No. 1, (2008), 144-147. (https://doi.org/10.1039/B802363H).
38. Kim, H.J., Park, H.S., Hyun, M.S., Chang, I.S., Kim, M. and Kim, B.H., "A mediator-less microbial fuel cell using a metal reducing bacterium, Shewanella putrefaciens", ***Enzyme and Microbial Technology***, Vol. 30, No. 2, (2002), 145-152. (https://doi.org/10.1016/S0141-0229(01)00478-1).
39. Wang, H. and Pilon, L., "Physical interpretation of cyclic voltammetry for measuring electric double layer capacitances", ***Electrochimica Acta***, Vol. 64, No. (2012), 130-139. (https://doi.org/10.1016/j.electacta. 2011.12.118).